Rare Metal Materials and Engineering
Volume 46, Issue 9, September 2017
Online English edition of the Chinese language journal

Available online at www.sciencedirect.com
ScienceDirect

Cite this article as: Rare Metal Materials and Engineering, 2017, 46(9): 2411-2416.

ARTICLE

Fatigue Lifetime of Laser-MIG Hybrid Welded Joint of 7075-T6 Aluminum Alloy by *in-situ* Observation

Zhang Yin[1], Song Xiping[1], Chang Liyan[1], Wu Shengchuan[2]

[1] State Key Laboratory for Advanced Metals and Materials, University of Science and Technology Beijing，Beijing 100083, China; [2] State Key Laboratory of Traction Power, Southwest Jiaotong University, Chengdu 610031, China

Abstract: The fatigue lifetime of the laser-MIG hybrid welded joint of 7075-T6 aluminum alloy was studied by in-situ observation. The results show that there exists a strong relationship between the fatigue crack initiation lifetime and fatigue failure lifetime. For the base metal specimens the ratio of fatigue crack initiation lifetime and fatigue failure lifetime is about 64.5%, while for the welded joint specimens it is about 20.2%. The observation of fatigue fracture surface indicates that there are a large number of dimples in the base metal specimens, while lots of gas porosities appear in the welded joint specimens instead. These gas porosities are regarded to be the reason of lower fatigue crack initiation lifetime.

Key words: aluminum alloy; welded joint; *in-situ* observation; fatigue lifetime

7075-T6 aluminum alloy is a heat-treatable aluminum alloy with low density, moderately high strength, excellent corrosion resistance and good processing performances. It has been widely used in the transport industry, and is one of the most important structural materials in the aerospace industry[1-5]. Elimination of fasteners in these components by welding would provide considerable mass savings and a reduction in manufacture cost. In aluminum alloy welding, traditional methods are to join the components through arc welding or laser welding. However, arc welding cannot meet the needs of modern welding industries due to the wider heat-affected zone and the greater thermal stress after welding[6-8]. While for laser welding, the low melting-point elements in aluminum alloy are easily vaporized and lost from the weld region, leading to the formation of gas porosity, cracking susceptibility, changes of composition and mechanical properties, and other defects[9-12].

Laser-metal inert gas (MIG) hybrid welding is a combination of laser welding and arc welding, and has many advantages over laser welding or arc welding, such as elimination of undercut, prevention of porosity formation and modification of weld compositions[13-15]. S. C. Wu et al.[16] studied the laser-MIG hybrid welded joint of 7075-T6 aluminum alloy by means of high-resolution synchrotron radiation X-rays. They found that the strength loss of welded joint was due to the excessive evaporation of elemental Zn and the significant inverse segregation of elemental Cu in central fusion welds, whereas the gas porosity has little influence on the static strength of hybrid welds. Yan Jun et al.[17] studied the effect of welding wires on microstructure and mechanical properties of an aluminum alloy in CO_2 laser-MIG hybrid welding, and found that the tensile strength and elongation of welds decreased due to the formation of eutectic phases in fusion zone. Yan Shaohua et al.[18,19] investigated the microstructures, mechanical properties and fatigue strengths of laser-MIG hybrid welded joint of aluminum alloy. They found that the fatigue strength of the laser-MIG hybrid welded joint was better than that of the MIG welded joint, and by the fatigue fracture surfaces analysis, it was found that gas porosity was the main reason for the decrease of the fatigue strength of the hybrid welded joint. It is noteworthy that there are few reports on the fatigue crack initiation and propagation behavior of laser-MIG hybrid welded joint of 7075-T6 aluminum alloy, especially the

Received date: September 06, 2016
Foundation item: National Natural Science Foundation of China (21171018, 51271021)
Corresponding author: Song Xiping, Ph. D., Professor, State Key Laboratory for Advanced Metals and Materials, University of Science and Technology Beijing, Beijing 100083, P. R. China, Tel: 0086-10-62333213, E-mail: xpsong@skl.ustb.edu.cn

real-time observation of fatigue crack initiation and propagation behavior. In this research, fatigue crack initiation lifetimes and fatigue failure lifetimes of base metal and welded joint of 7075-T6 aluminum alloy were studied by an *in-situ* fatigue method, and based on the experimental results, a new method was used to evaluate the fatigue lifetime of base metal specimens and welded joint specimens. In addition, the microstructure and fractography of base metal and welded joint were also studied. Some interesting results have been obtained.

1 Experiment

The laser-MIG hybrid welded joint of 7075-T6 aluminum alloy was used in this study. The 7075-T6 aluminum alloy plates with a thickness of 2 mm were cut into sheets of 240 mm × 60 mm. The filler wire was ER5356 (Φ1.2 mm). The chemical composition of 7075-T6 aluminum alloy and filler wire are given in Table 1. Before welding, the joint surfaces were abraded with sandpaper in order to remove any dirt or grease adhering to the surface. The direction of welding was parallel to the rolling direction. Laser-MIG hybrid welding was performed by incorporating a fiber laser (YLR-4000) with a gas metal arc welding (GMAW, Fronius TPS4000) power source. The 99.999% pure argon gas with a flow rate of 45 L·min^{-1} was selected as the shielding gas. To avoid reflection, the laser was inclined by approximately 10 degree, and the arc torch was inclined by 70 degree with the sample plane. Detailed parameters are listed in Table 2.

Fatigue specimens of welded joint were cut from the welded plate. The cutting position and dimensions are shown in Fig.1. The fusion zone of welded joint was adjusted to be at the middle of the gauge section during cutting. The fatigue specimens of base metal were cut from the primary plate with the same dimension of welded joint specimens. All the specimens were mechanically polished for the *in-situ* fatigue observation. The microstructures of both welded joint and base metal were examined by optical microscopy. The optical microscopy specimens were prepared with a standard metallographic technique and were etched with Keller's reagent (2 mL HF, 3 mL HCl, 5 mL HNO_3, and 190 mL H_2O).

The *in-situ* fatigue tests were carried out in the vacuum chamber of SHIMADZU SS-550 with a specially designed servo-hydraulic fatigue machine for fatigue loading. The stress-controlled tension–tension fatigue tests with a sinusoidal waveform signal (stress ratio R = 0.1, frequency=10 Hz) were conducted in vacuum (10^{-4} MPa) at room temperature. The loading frequency can be changed from 10 Hz to 0.10 Hz when recording. The fatigue crack initiation lifetimes and fatigue failure lifetimes of the specimens under the peak stress were recorded. Fatigue fractured morphology of various specimens was examined by a scanning electron microscope (SEM).

2 Results and Discussion

2.1 Microstructures

Fig.2 shows optical micrographs of laser-MIG hybrid welded joint of 7075-T6 aluminum alloy. The fine texture microstructure of base metal has been observed and many second-phase particles are found to uniformly distribute at the grain boundaries or inside the grain in base metal (Fig.2a). Affected by welding thermal cycle, grains and precipitates coarsen in HAZ, as seen in Fig.2b. A dendritic microstructure is found in the center of fusion zone, as shown in Fig.2c, which is due to the high cooling rate. The microstructural gradient in the laser-MIG hybrid welding method could influence the mechanical performances of welded joint, especially the fatigue performance.

2.2 *In-situ* observation of fatigue crack initiation and propagation

Fatigue damage in metals mainly includes the process of the initiation and propagation of micro-cracks. Fatigue crack initiation and propagation behaviors of base metal and laser-MIG hybrid welded joint of 7075-T6 aluminum alloy are displayed in Fig.3 and Fig.4, respectively. Fig.3 illustrates a typical case of fatigue micro-crack initiation and propagation behavior of base metal (loading direction is parallel to rolling direction) under the applied loading of σ_{max}=490 MPa. Fig.3a shows that there is no crack on the surface of plate specimen. From Fig.3b, it is observed that the first fatigue crack (marked as 1) appears as the cyclic number reaches 73713 cycles. This cyclic number is defined as fatigue crack initiation lifetime (N_i). With the increase of cyclic numbers, as shown in Fig.3c, multiple micro-cracks initiate at the immediate vicinity of the second phase particles (marked as 2 and 3). Then the fatigue

Table 1 Chemical composition of 7075-T6 and wires ER5356 (wt%)

Alloy	Zn	Mg	Cu	Ti	Mn	Cr	Fe	Si	Al
7075-T6	5.54	2.43	1.30	0.05	0.10	0.19	0.25	0.20	Bal.
ER5356	0.10	4.80	0.10	0.12	0.15	0.10	0.40	0.20	Bal.

Table 2 Parameters of laser-MIG hybrid welding

Power/kW	Current/A	Voltage/V	Touch speed/m·min^{-1}	Filler speed/m·min^{-1}	Defocusing distance/mm
2.9	110	18	2.5	6.5	-1

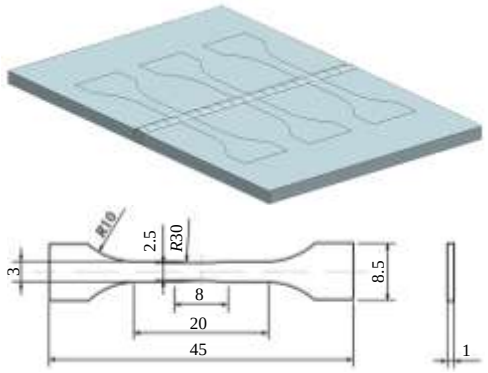

Fig.1 Cutting position and dimension of welded joint specimens used in this study

cracks grow continuously, passing through the metal/particle interface. It can be found that with further increase of cyclic number, the length and width of fatigue cracks increase significantly, as shown in Fig.3d.

Typical observations on initiation characteristics of fatigue crack of laser-MIG hybrid welded joint of 7075-T6 aluminum alloy are shown in Fig.4, which presents how a dominant crack forms under the applied loading of σ_{max}=300 MPa as the number of fatigue cycle increase. At the beginning of the fatigue no crack is observed, instead some gas porosities are observed (Fig.4a), implying that this section belongs to the fusion zone of welded joint. After 6313 cycles, the first initiation crack is observed, as shown in Fig.4b (marked as "1"). This cyclic number is regarded as the fatigue crack initiation lifetime of this specimen. With the increase of cyclic number, a new fatigue crack (marked as "2") which is perpendicular to the loading direction initiates and grows to be a main crack (Fig.4c). In the process of fatigue crack propagation, there is no other crack initiated and the main crack propagates in the two opposite directions perpendicular to the loading direction, as shown in Fig.4d.

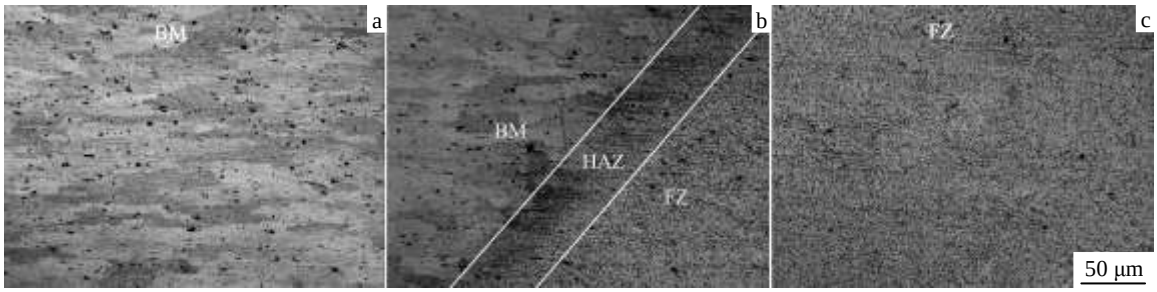

Fig.2 Optical micrographs of welded joint of 7075-T6 aluminum alloy: (a) BM-base metal, (b) HAZ-heat affected zone, and (c) FZ-fusion zone

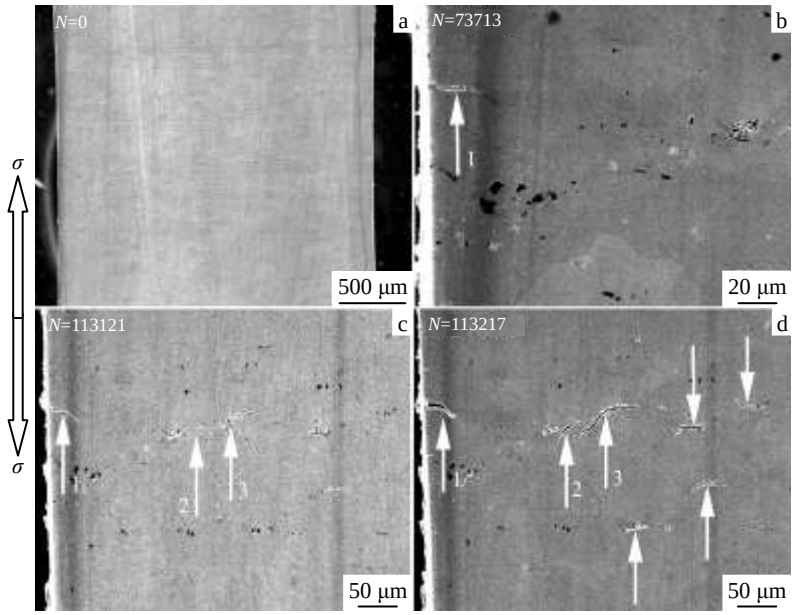

Fig.3 *In-situ* observation of fatigue crack initiation of base metal (σ_{max}=490 MPa): (a) 0 cycle, (b) 73713 cycles, (c) 113121 cycles, and (d) 113217 cycles

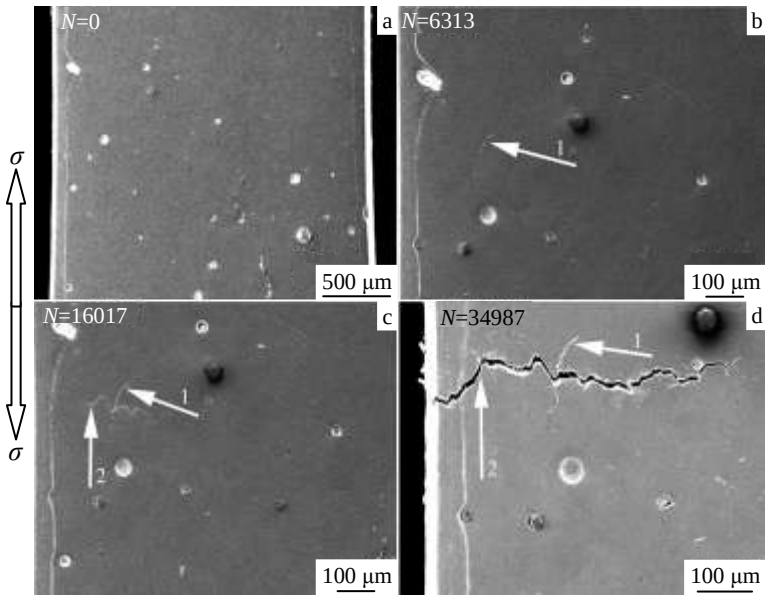

Fig.4 *In-situ* observation of fatigue crack initiation of welded joint (σ_{max}=300 MPa): (a) 0 cycle, (b) 6313 cycles, (c) 16017 cycles, and (d) 34987 cycles

The fatigue crack initiation lifetime (N_i) and fatigue failure lifetime (N_f) of base metal and welded joint under different stresses are displayed in Fig.5. Under this experimental condition, it has been found that there exists a strong relationship between the fatigue crack initiation lifetime and fatigue failure lifetime. The ratios of fatigue crack initiation lifetime to fatigue failure lifetime of base metal specimens and welded joint specimens are constant, i.e. 64.5% and 20.2%, respectively.

2.3 Fatigue lifetime

The *S-N* curves originated by the fatigue tests data of base metal specimens and laser-MIG hybrid welded joint specimens are displayed in Fig.6. The fatigue failure lifetimes of base metal and welded joint vary within a low scatter band. The scatter band of welded joint specimens is wider than that of base metal due to inhomogeneous microstructure of welded joint, which results from welding thermal process. Experimental results show that fatigue strength of base metal specimens is

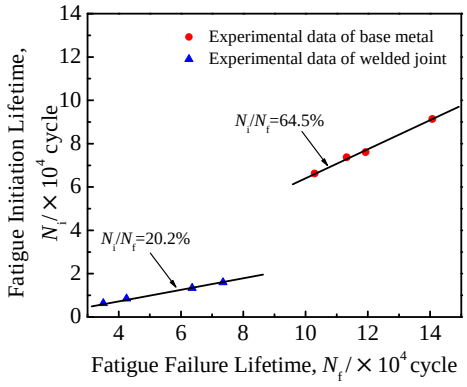

Fig.5 Ratios of N_i/N_f of base metal and welded joint

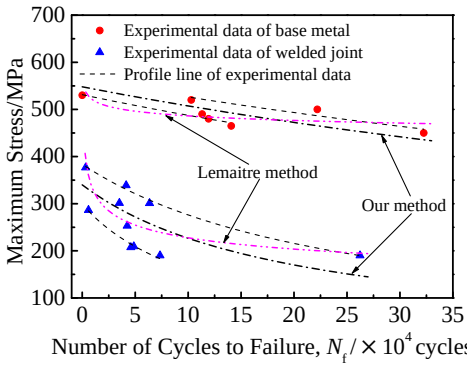

Fig.6 Experimental data and predicted fatigue lifetime curves of base metal and welded joint

higher than that of the laser-MIG welded joint specimens. It was reported that dendrite structure occurred in the fusion zone due to welding, leading to a drastic decrease of the mechanical behavior[20]. So the fine texture microstructure of base metal and many second-phase particles uniformly distributed at the grain boundaries or inside the grains leads to better fatigue performance than welded joint.

In this paper, a continuum damage mechanic model developed by Lemaitre[21] is used for predicting the fatigue lifetimes of base metal and welded joint of 7075-T6 aluminum alloy. Applied Lemaitre model to the one-dimensional case, stress ratio R=0.1, the fatigue lifetimes of base metal (N_{fB}) and laser-MIG hybrid welded joint (N_{fW}) can be predicted as follows:

$$N_{fB} = 2.91\times10^{97}\sigma_{max}^{-34.41} \quad (1)$$

$$N_{fW} = 4.29\times10^{20}\sigma_{max}^{-6.21} \quad (2)$$

According to the profile line of the experimental data, a new fatigue lifetime predication method is proposed. The fatigue lifetime formulas of base metal (N'_{fB}) and laser-MIG hybrid welded joint (N'_{fW}) can be predicted as follows:

$$N'_{fB} = 6.85\times10^{8}\sigma_{max}^{-1} - 1.25\times10^{6} \quad (3)$$

$$N'_{fW} = 6.80\times10^{7}\sigma_{max}^{-1} - 2.0\times10^{5} \quad (4)$$

The predicted results of two methods are shown in Fig.6. Comparing these two methods it is found that the prediction method based on the profile line is closer to the experimental results, whereas the prediction method based on the Lemaitre method is not in good agreement with the experimental data. So it is reasonable to believe that the prediction method by profile line has a strong ability in predicting fatigue lifetime in this experiment. Due to these formulas for fatigue lifetime prediction obtained under certain experimental conditions, more experimental data will be needed for confirmation in the further study.

2.4 Fatigue fracture morphology

Fig.7 shows the fatigue fracture surface of the base metal specimen tested at σ_{max}=490 MPa. Fig.7a displays the overall morphology, which is composed of distinct fatigue fracture feature and static tensile fracture feature. Fine dimples, tear ridge and micro-void are observed on fracture surface, and shallow straight striations are also observed (marked as A). Fig.7b shows two different types of dimples, some close to the voids and some associated with the second phase coarse particles. The dimples on the fracture surface indicate a ductile type failure. In the base metal morphology, many uniformly distributed second phase particles, which are also found in the optical micrograph (Fig.2a), have fallen off the base metal because of the fracture process. The size of second phase particles is 1~5 μm. Generally, fine and uniformly distributed second phase particles hinder the fatigue crack propagation.

The fracture surface of welded joint, however, is quite different from that of base metal. Fig.8 shows the fracture surface features of laser-MIG hybrid welded joint tested at σ_{max}=300 MPa. Many gas porosities with different sizes are observed to distribute randomly on the fracture surface, and the maximum diameter of these gas porosities is about 120 μm, as pointed out by the arrow in Fig.8b. These gas porosities which produced during the welding process act as defects during the fatigue and as a result promote the initiation and propa- gation of fatigue crack.

Fatigue fracture of laser-MIG hybrid welded joint and base metal of 7075-T6 aluminum alloy are affected by many factors. Gas porosity is the key factor causing fatigue fracture of welded joint. Gas porosities formed during welding may cause inhomogeneous plastic deformation and local stress concentration in the welded joint. And stress concentration deteriorates local mechanical properties of welded joint[22-24]. It was reported that the number of gas porosities per unit volume and the gas porosity size distribution were major factors controlling the fatigue lifetime and its scatter[25]. Compared to welded joint, base metal has no gas porosities, but has many second phase particles instead which are distributed homogeneously inside the base metal. Since the size of second phase particles is smaller than that of gas porosity, and is in a high degree of uniformity, they would promote the less local strain accumulation and stress concentration, which could lead to the superior fatigue strength of base metal compared with that of the welded joint.

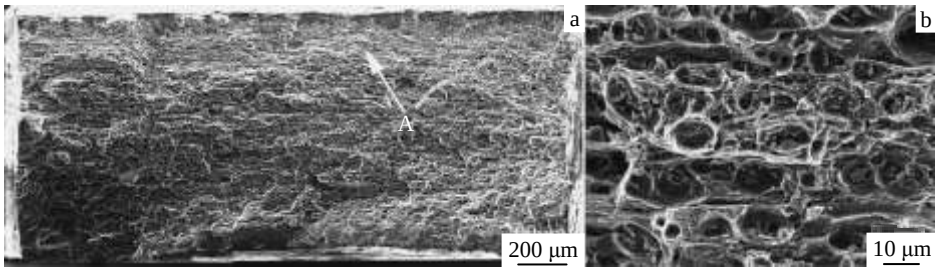

Fig.7 Fatigue fracture micrographs of base metal of 7075-T6 aluminum alloy

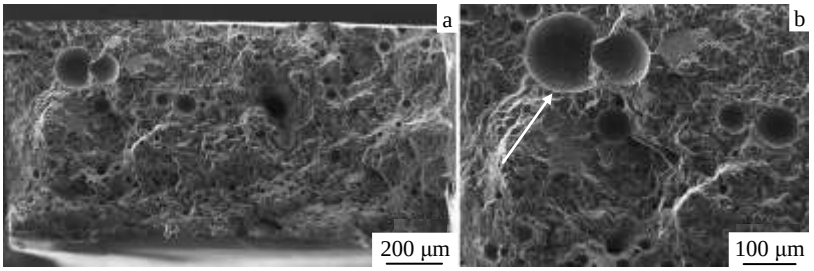

Fig.8 Fatigue fracture micrographs of welded joint of 7075-T6 aluminum alloy

3 Conclusions

1) The fatigue crack initiation lifetimes of base metal and laser-MIG hybrid welded joint of 7075-T6 aluminum alloy are obtained by *in-situ* observation. The ratios of fatigue crack initiation lifetime to fatigue failure lifetime of base metal and welded joint of 7075-T6 aluminum alloy are 64.5% and 20.2%, respectively.

2) The fatigue lifetime prediction formulas of base metal and welded joint have been obtained based on the profile line prediction method. They are as follows:

$N'_{\mathrm{fB}} = 6.85\times10^{8}\sigma_{\max}^{-1} - 1.25\times10^{6}$

$N'_{\mathrm{fW}} = 6.80\times10^{7}\sigma_{\max}^{-1} - 2.0\times10^{5}$

3) Fatigue fracture surface of base metal has many dimples, while fracture surface of welded joint has many gas porosities of different sizes. For welded joint, gas porosity is the main factor affecting fatigue crack initiation, and the main reason for the decrease of the fatigue strength of welded joint of 7075-T6 aluminum alloy.

References

1 Su Xin, Li Mengnan, Zhang Aiping *et al*. *Rare Metal Materials and Engineering*[J], 2014, 43(10): 2354 (in Chinese)

2 Hu B, Richardson I M. *Materials Science and Engineering A*[J], 2007, 459(1-2): 94

3 Liu Cheng, Northwood D O, Bhole S D. *Materials and Design*[J], 2004, 25(7): 573

4 Su Xin, Liu Tan, Xu Guangming. *Rare Metal Materials and Engineering*[J], 2015, 44(3): 0581 (in Chinese)

5 Li Ling, Shen Luming, Proust Gwénaëlle. *Mechanics of Materials*[J], 2015, 81: 84

6 Ravindra B, Kumar T S, Balasubramanian V. *Transactions of Nonferrous Metals Society China*[J], 2011, 21(6): 1210

7 Lu Yi, Chen Shujun, Shi Yu *et al*. *Journal of Manufacturing Processes*[J], 2014, 16(1): 93

8 Zhao Y B, Lei Z L, Chen Y B *et al*. *Materials and Design*[J], 2011, 32(4): 2165

9 Chang C C, Chou C P, Hsu S N *et al*. *Journal of Materials Science & Technology*[J], 2010, 26(3): 276

10 Tani Giovanni, Campana Giampaolo, Fortunato Alessandro *et al*. *Applied Surface Science*[J], 2007, 253(19): 8050

11 Tsay L W, Shan Y P, Chao Y H *et al*. *Journal of Materials Science*[J], 2006, 41(22): 7498

12 Kim B H, Kang N H, Oh W T *et al*. *Journal of Materials Science & Technology*[J], 2011, 27(1): 93

13 Zhou J, Tsai H L. *International Journal of Heat and Mass Transfer*[J], 2008, 51(17-18): 4353

14 Matteï Simone, Grevery Dominique, Mathieu Alexandre *et al*. *Optics & Laser Technology*[J], 2009, 41: 665

15 Campana G, Ascari A, Fortunato A *et al*. *Applied Surface Science*[J], 2009, 255: 5588

16 Wu S C, Yu X, Zuo R Z *et al*. *Welding Journal*[J], 2013, 92: 64

17 Yan Jun, Zeng Xiaoyan, Gao Ming *et al*. *Applied Surface Science*[J], 2009, 255(16): 7307

18 Yan Shaohua, Nie Yuan, Zhu Zongtao *et al*. *Applied Surface Science*[J], 2014, 298: 12

19 Yan Shaohua, Chen Hui, Zhu Zongtao *et al*. *Materials and Design*[J], 2014, 61: 160

20 Cavaliere P, Nobile R, Panella F W *et al*. *International Journal of Machine Tools & Manufacture*[J], 2006, 46(6): 588

21 Lemaitre Jean. *Nuclear Engineering and Design*[J], 1984, 80: 233

22 Tagawa Tetsuya, Tahara Kazunori, Abe Eiji *et al*. *Welding International*[J], 2014, 28(1): 21

23 Zhang Fei, Su Xuekuan, Chen Ziyong *et al*. *Materials and Design*[J], 2015, 67: 483

24 Liu H, Shang D G, Guo Z K *et al*. *Fatigue & Fracture of Engineering Materials & Structures*[J], 2014, 37: 937

25 Buffière J Y, Savelli S, Jouneau P H *et al*. *Materials Science and Engineering A*[J], 2001, 316(1-2): 115

7075-T6 铝合金激光-MIG 复合焊焊接接头疲劳寿命原位研究

张 寅[1]，宋西平[1]，常丽艳[1]，吴圣川[2]

(1. 北京科技大学 新金属材料国家重点实验室，北京 100083)

(2. 西南交通大学 牵引动力国家重点实验室，四川 成都 610031)

摘 要：对 7075-T6 铝合金激光复合焊焊接接头的疲劳寿命进行了探究。结果表明：疲劳裂纹萌生寿命与疲劳寿命之间存在着一定的比例关系。对于母材试样，该比值为 64.5%；而对于焊接接头试样，该比值为 20.2%。疲劳断口表面观察发现，母材试样的疲劳断口上存在大量韧窝，而焊接接头试样疲劳断口上存在许多气孔。这些气孔被认为是引起焊接接头疲劳裂纹萌生寿命急剧下降的主要原因。

关键词：铝合金；焊接接头；原位观察；疲劳寿命

作者简介：张 寅，男，1991 年生，博士，北京科技大学新金属材料国家重点实验室，北京 100083，电话：010-62333213，E-mail: yinzhang330@163.com